Pergamon

Cement and Concrete Research 30 (2000) 281–289

CEMENT AND CONCRETE RESEARCH

Influence of degree of saturation on the borehole sealing performance of an expansive cement grout

Haluk Akgün[a,*], Jaak J.K. Daemen[b]

[a]*Department of Geological Engineering, Middle East Technical University, Ankara 06531, Turkey*
[b]*Mining Engineering Department, Mackay School of Mines, University of Nevada-Reno, Reno, NV 89557-0139, USA*

Received 2 May 1999; accepted 22 November 1999

Abstract

The strength measures of expansive cement grout borehole plugs cast in welded tuff cylinders is investigated as a function of the degree of saturation of the plugged rock cylinder and of borehole size. Details on experimental procedure regarding rock cylinder and cement grout preparation, sample curing conditions, experimental apparatus, sample loading, mechanical characterization of the rock, and cement grout, along with procedures for the determination of the sample saturation assuming uniform saturation, and strength measures are presented. The extrapolated axial strengths to a plug radius of 100 mm show that the more saturated samples show higher strengths as compared to the dry samples. The strength measures decrease with increasing plug radius, obeying a power law.

Keywords: Bond strength; Push-out strength; Cement paste; Expansion; Radioactive waste

1. Introduction

Materials used to seal a radioactive waste repository constitute an essential component of the repository system. Cementitious materials (cements, grouts, concretes) have been used in underground sealing in the oil, gas, and mining industries, as well as in other underground storage facilities [1–3]. According to various reports [3–10] major requirements for the repository seal materials include the following: The materials should (a) be mechanically adequate; (b) be well-bonded to the host rock; (c) provide a very low permeability to fluids, particularly in the interfacial zone between the seal material and host rock; (d) be stable and chemically durable; (e) be compatible with the surrounding rock; (f) be resistant to destructive expansion and cracking; and (g) be resistant to radionuclide transport. Some authors argue that repository seal materials should maintain their integrity for periods comparable to the life of the rock formations in which they are emplaced [7–9]. Hence, the seal should bond to the rock and should exclude fluid flow for some (as yet rather uncertain, but considerable) time.

Cementitious materials, because of their engineering properties combined with their potential for long-term geochemical stability, may satisfy the above requirements. Concretes discovered in the remains of many ancient structures have maintained their mechanical integrity and can function in their intended capacity today. Despite centuries of use and exposure to adverse environmental conditions such as atmospheric carbon dioxide, dissolved species in ore treatment liquids, and warm climatic conditions, such materials have endured better than the natural stone or brick found in the same structures [11–13]. During an investigation of the Troy Lock and Dam, New York, a core containing part of a metal anchor grouted into the foundation rock was recovered [14]. The 63-year-old grout, which remained continuously below the water table, provided an opportunity to study the effect of an adverse environment on the longevity (phase composition and microstructure) of the grout. X-ray diffraction (XRD), scanning electron microscopy (SEM) studies, and visual examinations showed that the adverse environmental conditions have not had a significant effect on grout composition or microstructure and that the grout/anchor bond was tight. Buck and Burkes [15] petrographically examined a 17-year-old grout specimen surrounded by rock salt. The grout contained Class C cement, brine, and calcium chloride. The conclusion was that the grout/rock salt inter-

* Corresponding author. Tel: +90-312-210-5727; fax: +90-312-210-1263.
E-mail address: hakgun@metu.edu.tr (H. Akgün)

0008-8846/00/$ – see front matter
PII: S0008-8846(99)00246-X

face was tight. The XRD and SEM analyses also showed that the composition and microstructure of the grout was normal.

A cementitious seal can develop mechanically or chemically. Mechanical bonding is established once the matrix hardens and can be enhanced by using expansive cement formulations. From that point, the cement plug must remain firmly in place against the host rock to prevent annular separation, at least until chemical bonding is established (i.e., so that no undesirable phase changes take place). Hence, the interface (bond) strength along the cement plug/rock contact is one indicator of the mechanical and chemical compatibility between these materials and is considered a critical element for the integrity of the seal system [16–24]. The interface should be strong enough to resist a site-specific water pressure (e.g., 1.85 MPa at the Waste Isolation and Pilot Plant (WIPP) site [25]; 11 MPa at the Gorleben site [26]) without shear failure. The interface shear strength should exceed all reasonably calculated requirements [21–24,27,28] and should be investigated as a function of time, pressure, temperature, and groundwater conditions [29].

The work described herein is part of a research effort on sealing man-made openings in the welded tuff formations at Yucca Mountain, Nevada. The U.S. Department of Energy (USDOE) has proposed this site as the candidate high-level radioactive waste repository site in the United States. Testing was performed on rock specimens taken from the densely welded brown unit of the Apache Leap tuff near Superior, Arizona. The main reason for selecting Apache Leap tuff included the fact that Apache Leap tuff is fairly similar mineralogically, geochemically, and mechanically to some of the welded tuff formations at Yucca Mountain [19,30]. The objective of this study is to determine the bond strength of cement grout borehole plugs cast in welded tuff cylinders as a function of the degree of saturation of the plugged rock cylinder and of borehole size. The bond strength is determined through push-out testing that involves the use of a steel rod to experimentally dislodge a cement grout plug emplaced within the coaxial borehole of a hollow rock cylinder. Some seals at Yucca Mountain, quite possibly the major ones, are likely to be emplaced in an unsaturated rock mass. Since it is not obvious what the consequences of this might be for seal performance, this study includes testing of seal performance as a function of the degree of saturation of the push-out specimens through curing the samples in a controlled environment (e.g., in an environmental chamber) with the assumption that the degree of saturation throughout the push-out specimen (i.e., within the cement plug and the tuff core) is uniform. The push-out tested tuff cylinders had inside radii ranging from 6.35 to 50.80 mm, outside radii from 38.10 to 93.66 mm, and lengths from 71.50 to 213.2 mm. The tuff cores were plugged with nearly centered cement grout plugs having length-to-radius ratios of approximately 2.0 and stored in dry, low, or medium saturated conditions for 8 days prior to push-out testing. The expandable cement grout formulation was Self-Stress II cement grout. The researchers were prohibited through a contract with the cement manufacturer to investigate the chemical composition of the cement and of the grout, to study the details of the microstructure, to microscopically characterize the grout, etc. The cement grouts of the push-out specimens were initially loaded to 4450 N. The load was kept approximately constant and incremented 4450 N every 2 min until the plug failed. The load and displacements were recorded every 30 s until failure.

2. Methods

2.1. Rock cylinder preparation

Cylindrical push-out test specimens were neatly cored from welded tuff blocks. A 6.35-mm radius central hole was neatly cored in push-out cylinders with an outside radius of 38.1 mm, a 12.7- or 25.4-mm radius central hole in cylinders with an outside radius of 76.2 mm, and a 50.8-mm radius central hole in cylinders with a 93.66-mm outside radius. The sample ends were ground flat to 0.025 mm. A straightedge was used to check that the specimen bottom ends did not depart from perpendicularity to the axis of the specimen by more than 0.025 degrees (approximately 0.25 mm in 51 mm) according to ASTM [31]. The cored tuff cylinders were kept in the oven for a week at 100 to 105°C; removed, weighed for the determination of the weight of the dry tuff solids, and allowed to cool for approximately 4 h prior to plugging.

2.2. Cement grout preparation

The type of cement used was Ideal Type I/II cement, and is referred to as Self-Stress II. Self-Stress II cement is composed of Ideal Type I/II Portland cement (from Tijeras Canyon, NM), mixed with 50% distilled water, 10% D53 (an expansive agent), and 1% D65 (a dispersant). All percentages are weight percent with respect to cement and all additives are trademarks of the cement manufacturer. The cement grout mixing for the borehole plugs was performed according to American Petroleum Institute [32]. Cement (333 g) and distilled water (150 g) were weighed. The water was poured into the mixing container and the cement was added to the water in not more than 15 s (while the mixer speed was on two). After all the cement was added, the slurry was mixed at speed six for an additional 35 s. During this mixing, any paste that collected on the sides of the mixing container was scraped with a spatula. A rubber stopper was placed into the inner borehole of the tuff cylinder at a level where a cement plug was to be located. The cement slurry was poured onto the rubber stopper by means of a funnel and plastic tube with minimum time lag (i.e., in less than 30 s), yet sufficiently slow to avoid violent turbulence. The bottom end of the plastic tube was submerged in the slurry. The funnel and tube were raised as the cement slurry level increased. Care was taken to minimize turbulence as much as possible during pouring in an attempt to prevent the occurrence of air voids within the set cement. Pouring was stopped when the desired plug length was obtained. The pouring time was measured and recorded. A thin layer of water

was poured on top of the cement plug 15 min after cement mixing to prevent cement drying.

2.3. Push-out sample curing conditions, experimental apparatus, and sample loading

The plugged push-out specimens were placed into the environmental chamber or underwater 1 h after cement pouring and cured at an ambient room temperature of 24 ± 2°C for a period of 8 days prior to initiating testing. The cement plugs of the medium saturated push-out specimens were cured under water. The cement plugs of the dry and low saturated push-out samples were cured in an environmental chamber at relative humidities of 45 and 80%, respectively. A rubber stopper was placed tightly in the top boreholes of the low saturated samples prior to placing them into the environmental chamber. The rubber stopper prevented the evaporation of water on top of the cement plugs, which might have led to cracking. The dry samples were placed in the environmental chamber without a rubber stopper in the top boreholes in an attempt to investigate the drying effect on cement plugs. On the seventh day of cement curing, the top end of the cement plugs were ground with a blind bit and the samples were put back into their curing environments. On the eighth day, the rubber stoppers were removed from the bottom ends of the cement plugs and bottom vertical bars encapsulated in plastic anchors were screwed into the plug bottoms. A horizontal arm was attached to the bottom vertical bar. A linear variable differential transducer (LVDT) and a dial gage were installed to the horizontal arm of the bottom vertical bar to measure the bottom cement plug displacement during push-out testing.

Fig. 1 shows the push-out test setup. A cylindrical steel rod applied an axial load to a cement grout plug installed in a rock cylinder. The top and bottom displacements of the borehole plug were measured with two LVDTs. The axial load was measured with a compression load cell. A data acquisition system was used to record the applied load, cement plug top and bottom axial displacement, and ambient room temperature. Two dial gages were used to measure the top and bottom cement plug displacements manually, thus providing a check on the automatically recorded data. A compression machine with a dial indicator applied the axial load.

A cylindrical steel plate was centered on the bottom bearing plate of the compression machine. Three threaded steel rods were bolted vertically to the cylindrical plate. They were also clamped to each other to increase stability. Four horizontal arms were clamped to the vertical steel rods. The bottom LVDT and dial gage for measuring the bottom plug displacement were clamped to the two lowermost horizontal arms. The upper horizontal arms (machined flat on their upper surfaces) supported the top LVDT and dial gage that measured the top plug displacement. A circular steel platen was centered on the bottom cylindrical steel plate. The platen had a slit on one side to allow the downward movement of the horizontal arm of the bottom displacement monitoring rod. The horizontal arm was machined flat on the upper surface to support the bottom LVDT and dial gage. A square platen with a central hole was centered on the circular steel platen with a slit.

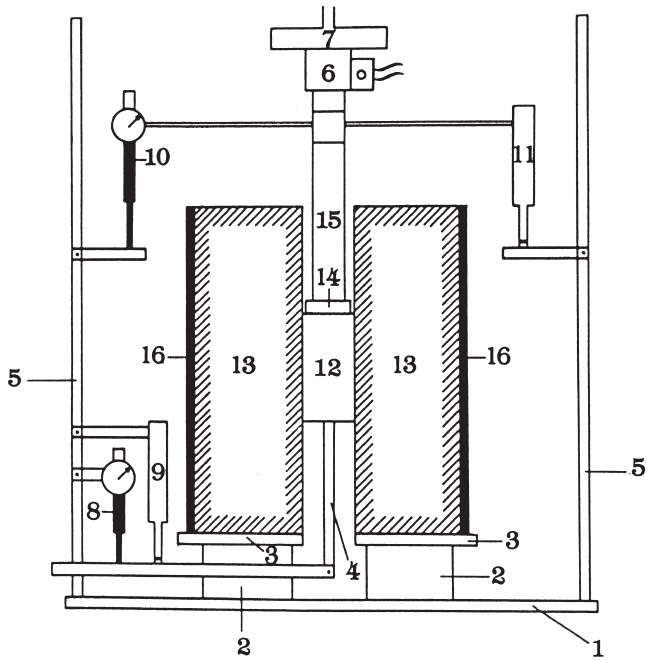

Fig. 1. Schematic drawing of push-out test setup 1. Cylindrical steel plate; 2. Circular steel plate with a slit; 3. Square steel plate; 4. L-shaped steel rod; 5. Vertical steel rods; 6. Load cell; 7. Loading platen; 8, 10. Dial gages; 9, 11. LVDTs; 12. Cement grout plug; 13. Rock sample; 14. Steel cylinder; 15. Axial bar; 16. Steel pipe.

The push-out sample was placed centrally on the square steel platen. A steel disc with a thickness of 6.35 mm and diameters of 12.0, 24.1, 48.3, or 99.1 mm (depending on the plug diameter) was centered on top of the cement plug. Particular care was taken so that the steel disc did not touch the inner borehole to prevent any annular friction. Cylindrical steel rods with lengths of 127 mm and diameters of 10.16, 20.32, 41.66, or 85.60 mm (depending on the plug diameter) was centered on the thinner disc to transmit the axial load to the plug. Two circular jackets with horizontal arms were clamped around the loading rod to install the top LVDT and top dial gage. The applied axial load was measured by the load cell in between the cylindrical axial bar and the loading platen. A steel pipe was placed around the specimens to provide confinement.

The sample was initially loaded to 4450 N (1000 lbf) with care taken to keep the load constant by adjusting the loading knob. The load and top and bottom plug displacements were recorded manually at 30-s intervals for 2 min while the data acquisition system was programmed to collect data every 10 s. The procedure was repeated by adding load increments of 4450 N (1000 lbf) every 2 min until the sample failed. Upon failure, the load and displacements were recorded every 15 s while the time increment in the data acquisition system was changed to collect data every second.

3. Mechanical characterization of samples

3.1. Cement slurry viscosity and density measurements

Table 1 presents the results of four viscosity and density measurements. The viscosity was measured with a FANN 35A/SR 12 viscometer, manufactured by FANN Instrument Co., Houston, Texas, USA. Viscosity and density measurements were taken at a room temperature of 27°C, relative room humidity of 50 ± 1% and at atmospheric pressure. The viscosity of the cement slurry varied from 32×10^{-3} kg/m s (32 centipoises) at 300-rpm rotor speed to 200×10^{-3} kg/m s (200 centipoises) at 3 rpm. The average cement slurry density ± one standard deviation was determined to be 1.86 ± 0.013 g/cm^3.

3.2. Uniaxial compressive strength, Young's modulus, and Poisson's ratio

Eleven cylindrical samples were prepared by curing cement pastes in acrylic molds for 8 days. The nominal diameter and length were 50.8 and 127 mm, respectively. A compression machine was used to load the specimens at a loading rate of 252 N/s. The mean and standard deviation of the uniaxial compressive strength were 18.8 and 0.97 MPa, respectively. All samples experienced splitting failure. The failed specimens were observed to be free of air voids and showed a uniform dense composition. Three specimens were tested with a deformation jacket to determine the Young's modulus and Poisson's ratio of the cement. The mean Young's modulus (E_p) and mean Poisson's ratio (υ_p) ± one standard deviation of the Self-Stress II cement grout cylinders tested was 5254 ± 270 MPa and 0.22 ± 0.05, respectively [20]. The mean Young's modulus (E_r) and mean Poisson's ratio (υ_r) ± one standard deviation of five Apache Leap tuff cylinders tested was 22600 ± 5700 MPa and 0.20 ± 0.03, respectively [30].

4. Determination of sample degree of saturation

The degree of saturation of the push-out specimen is calculated with the assumption that the degree of saturation throughout the push-out specimen (i.e., within the cement plug and the tuff core) is uniform. Each batch of Self-Stress II cement mixture consists of 333 g of cement and 150 g of water. Of 333 g of cement, 300 g is dry cement solids, 30 g is D53 additive, and 3 g is D65 additive. The cement slurry mass (M_{ct}) is calculated as seen in Eq. (1):

$$M_{ct} = M_{cs} + M_{cw} + M_{ad} \tag{1}$$

where M_{cs} = mass of cement solids, M_{cw} = mass of cement water, and M_{ad} = mass of cement additives. Therefore, the mass proportions are $M_{cs} = 0.621\ M_{ct}$, $M_{cw} = 0.311\ M_{ct}$, and $M_{ad} = 0.0683\ M_{ct}$.

The mass of water (M_w) in the push-out specimen 8 days after curing in the desired environment is [see Eq. (2)]:

$$M_w = M_T - M_{ts} - M_{cs} - M_{ad} = M_T - M_{ts} - 0.6893\ M_{ct} \tag{2}$$

where M_T = total mass of the plugged push-out specimen and M_{ts} = mass of the tuff solids (determined after leaving the cored rock cylinder in the oven at 100 to 105°C for a week). Eq. (2) assumes that the void spaces of the oven-dried rock cylinder are dry after being left in the oven for a period of 1 week.

The volume of water (V_w) in the push-out specimen 8 days after curing in the desired environment follows from Eq. (2) [see Eq. (3)]:

$$V_w = \frac{M_w}{\rho_w} = \frac{M_T - M_{ts} - 0.6893\ M_{ct}}{\rho_w} \tag{3}$$

where ρ_w = density of water.

The volume of voids (V_v) in the push-out specimen is the sum of the volume of air (V_a) and the volume of water (V_w). The volume of air is calculated from Eq. (4):

$$\begin{aligned} V_a &= V_T - V_{ts} - V_{cs} - V_{ad} - V_w \\ &= V_r + V_c - V_{ts} - V_{cs} - V_{ad} - V_w \end{aligned} \tag{4}$$

where V_T = total volume of push-out specimen, V_{ts} = volume of tuff solids, V_{cs} = volume of cement solids, V_{ad} = volume of cement additives, V_r = volume of cored rock cylinder, and V_c = volume of cement plug.

The volume of voids in the push-out specimen can thus be expressed as seen in Eq. (5):

$$\begin{aligned} V_v &= V_a + V_w \\ &= V_r + V_c - V_{ts} - V_{cs} - V_{ad} \\ &= V_r + V_c - \frac{M_{ts}}{\rho_{ts}} - \frac{0.621\ M_{ct}}{\rho_{cs}} - \frac{0.0683\ M_{ct}}{\rho_{ad}} \end{aligned} \tag{5}$$

where ρ_{ts} = density of tuff solids, ρ_{cs} = density of cement solids, and ρ_{ad} = density of cement additives.

The average degree of saturation (S) of the push-out specimen is given by Eq. (6):

$$\begin{aligned} S &= \frac{V_w}{V_v} \times 100 \\ &= \frac{(M_T - M_{ts} - 0.6893\ M_{ct})/\rho_w}{\left(V_r + V_c - \frac{M_{ts}}{\rho_{ts}} - \frac{0.621\ M_{ct}}{\rho_{cs}} - \frac{0.0683\ M_{ct}}{\rho_{ad}}\right)} \times 100 \end{aligned} \tag{6}$$

Table 1
Viscosity and slurry density of Self-Stress II cement

Rotor speed (rpm)	Time after mixing cement (s)	Viscosity (kg/m s × 10^3)			
		Sample 1	Sample 2	Sample 3	Sample 4
300	60	35.50	35.00	35.50	32.00
200	80	37.50	36.80	37.50	33.00
100	100	42.00	42.00	42.00	37.50
6	120	112.5	112.5	112.5	112.5
3	140	200.0	200.0	200.0	200.0
Cement slurry density (g/cm^3)		1.87	1.85	1.84	1.86

5. Determination of strength measures

The bond strength or the average shear stress along the cement plug/rock interface at failure ($\tau_{av,f}$) is calculated from Eq. (7):

$$\tau_{av,f} = \frac{\sigma_{z,f}\, a}{2L} \tag{7}$$

where $\sigma_{z,f}$ is the axial strength or the axial stress applied to the plug at failure, a is the plug radius, and L is the plug length.

The peak shear strength or the peak shear stress at the loaded end (top) of the plug/rock interface at failure ($\tau_{p,f}$) is calculated as shown in Eqs. (8), (9), (10a), (10b), and (10c) [20]:

$$\tau_{p,f} = \frac{\sigma_{z,f}\lambda}{2\tan h[\lambda(L/a)]} \tag{8}$$

$$\lambda = \sqrt{\frac{1-2\upsilon_p(\mathrm{VSF})}{(1+\upsilon_r)(E_p/E_r)\ln(r_c/a)}} \tag{9}$$

$$\mathrm{VSF} = \frac{\upsilon_p(1-(a/R)^2)}{\{(1-\upsilon_p)[1-(a/R)^2]+(E_p/E_r)(1+\upsilon_r) \times [(1-2\upsilon_r)(a/R)^2+1]\}} \tag{10a}$$

$$r_c = a + [2.07e^{-0.18(E_p/E_r)}]L \qquad \text{if } R > r_c \tag{10b}$$

$$r_c = R \text{ if } (\quad R \leqslant r_c) \tag{10c}$$

where E_p/E_r is the ratio of the Young's modulus of plug and rock, υ_p and υ_r is the Poisson's ratio of plug and rock, respectively, r_c is the critical radius beyond which the shear stresses and axial displacements in rock are considered negligible, and R is the rock cylinder outside radius.

6. Push-out test results, discussion, and recommendations

Push-out tests were performed on 51 Apache Leap tuff cylinders plugged with nearly centered Self-Stress II cement plugs having length-to-radius ratios of about 2.0. The push-out cores were cured at dry, low, or medium saturated conditions following plugging as described previously. Table 2 gives the dimensions of the tested cylinders and summarizes the axial strength, bond strength, and peak shear strength. The axial strength, bond strength, and peak shear strength ranged from 8.00 to 62.40 MPa, 1.99 to 13.26 MPa, and 9.31 to 44.59 MPa, respectively. Samples showing high axial strength generally lead to high bond strengths and high peak shear strengths. Samples with higher degree of saturations and smaller inside diameters generally lead to higher strength measures.

In all tests the bottom plug axial displacements were smaller than the top plug axial displacements prior to bond failure. Upon plug slip, the difference between the top and bottom plug displacements decreased most probably due to stress relief caused by slip along the interface. Akgün and Daemen [20] present a typical stress-displacement curve. The plugs failed after periods ranging from 6 min to one-half hour. On the average, the residual axial strengths were about 17% of the peak axial strengths. The push-out stress-displacement behavior agreed with those reported by previous studies [16,17,19,20].

The mean degree of saturation in the dry, low, and medium saturated samples (prior to push-out testing) ± one standard deviation was calculated as 24.51 ± 16.77%, 34.83 ± 17.97%, and 56.29 ± 7.86%, respectively. The degree of saturation within the push-out specimens increased from dry to medium saturated samples and with increased plug radius (Tables 2 and 3). Self-Stress II is an expansive cement (i.e., a product that results in a cement grout that increases in volume during curing). During the hydration period, the cement grout needs to take in free water. Therefore, the increase in degree of saturation with increased plug radius (or plug volume) is attributed to the picking up of most of the free water by the cement grout rather than by the tuff cylinder. It is not surprising that the degree of saturation of the push-out samples is low. Although the porosity of tuff is fairly high, its permeability is extremely low. Unless special procedures are used (i.e., the application of differential water pressures), it is very unlikely that much water will penetrate into samples of this tuff, even if the samples are immersed in water.

Tables 4, 5, and 6 give the mean axial strength, mean bond strength, and mean peak shear strength as a function of the push-out sample uniform degree of saturation and plug radius. All three strength measures increased with increased degree of saturation and with decreased plug radius. There was no discernible difference between the strengths of the low and medium saturated samples. The dry samples showed lower strength measures than the more saturated samples. This paralleled conclusions from previous studies [33–35]. A common observation in these studies was that if the push-out samples were allowed to dry out, their cement plugs showed significant shrinkage and drastic strength reduction after moderately long periods of time (e.g., more than 2 years). The low saturated samples showed comparable strength measures to the medium saturated samples most probably because the cement plugs of these samples were not allowed to dry out (i.e., they were cured with a film of water remaining on top of their plugs during the entire 8-day cement curing period). Since the dry samples were cured without a thin film of water remaining on top of their plugs, this might have led to shrinkage and/or cracking along the plug/rock interfaces and to decreased strength measures.

Fig. 2 gives best-fit curves for the axial strength as a function of saturation condition and plug radius. The data in Table 2 are used to obtain the best-fit curves. The best-fit equations along with the correlation coefficients for medium saturated, low saturated and dry samples, respectively, are obtained from Eqs. (11), (12), and (13):

Table 2
Dimensions of the tuff cylinders used for push-out tests, the average degree of saturation (S), axial strength ($\sigma_{z,f}$), bond strength ($\tau_{av,f}$), and peak shear strength ($\tau_{p,f}$)

Sample #	a (mm)	R (mm)	L_r (mm)	L_h (mm)	L (mm)	S (%)	$\sigma_{z,f}$ (MPa)	$\tau_{av,f}$ (MPa)	$\tau_{p,f}$ (MPa)
M1	6.35	38.10	77.00	31.40	14.50	51.36	43.40	9.50	31.04
M2	6.35	38.10	77.30	34.10	14.20	52.10	43.40	9.70	31.05
M3	6.35	38.10	83.30	40.70	15.40	54.29	45.50	9.38	32.51
M4	6.35	38.10	79.10	34.20	13.70	48.94	43.40	10.06	31.08
M5	6.35	38.10	74.90	21.70	15.60	49.73	56.40	11.48	40.29
M6	6.35	38.10	75.30	35.40	13.40	51.66	43.40	10.28	31.10
M7	6.35	38.10	80.10	36.00	14.50	55.65	46.80	10.25	33.47
M8	6.35	38.10	77.90	34.20	15.30	54.12	53.80	11.16	38.44
M9	6.35	38.10	73.70	27.30	15.50	53.75	52.90	10.84	37.80
M10	6.35	38.10	71.50	21.20	13.50	51.32	56.40	13.26	40.41
M11	6.35	38.10	74.70	26.70	16.30	50.53	53.80	10.48	38.41
M12	6.35	38.10	73.70	23.90	16.30	56.60	55.50	10.81	39.63
M13	6.35	38.10	76.70	33.80	12.80	45.54	50.30	12.48	36.10
M14	6.35	38.10	91.70	44.00	15.30	50.71	62.40	12.95	44.59
M15	12.70	76.20	105.3	30.20	31.00	51.42	42.70	8.75	30.51
M16	12.70	76.20	115.1	33.50	30.70	51.45	35.20	7.28	25.15
M17	12.70	76.20	82.00	24.60	32.20	51.45	29.00	5.72	20.71
M18	12.70	76.20	100.1	33.50	30.10	58.93	35.10	7.40	25.09
M19	12.70	76.20	87.80	28.80	29.80	55.06	33.70	7.18	24.09
M20	12.70	76.20	99.00	27.90	29.30	59.10	35.30	7.65	25.24
M21	25.40	76.20	129.6	38.30	49.10	58.58	17.60	4.55	15.24
M22	25.40	76.20	102.9	15.30	43.60	65.99	28.50	8.30	24.75
M23	25.40	76.20	114.6	34.40	46.50	55.33	22.00	6.01	19.07
M24	50.80	93.66	186.9	45.80	101.2	73.00	15.40	3.87	17.92
M25	50.80	93.66	206.4	64.20	102.2	71.55	13.00	3.23	15.13
M26	50.80	93.66	133.3	6.30	87.60	74.41	16.20	4.70	18.86
L1	12.70	76.20	120.9	63.90	25.50	10.22	32.10	7.99	23.04
L2	12.70	76.20	111.9	35.90	25.40	30.86	29.70	7.43	21.32
L3	12.70	76.20	151.4	95.90	30.30	20.64	34.70	7.27	24.80
L4	12.70	76.20	128.5	44.70	29.10	16.47	32.10	7.00	22.96
L5	12.70	76.20	170.5	83.10	32.50	13.66	48.60	9.50	34.70
L6	12.70	76.20	132.6	58.40	31.30	18.96	30.70	6.23	21.93
L7	12.70	76.20	172.0	82.50	29.00	14.00	34.60	7.58	24.75
L8	25.40	76.20	157.9	57.40	52.60	25.31	33.40	8.06	28.89
L9	25.40	76.20	141.4	61.30	49.90	29.13	31.60	8.04	27.35
L10	25.40	76.20	171.2	65.20	50.30	26.09	24.10	6.08	20.86
L11	25.40	76.20	172.1	61.10	49.70	26.48	29.60	7.56	25.62
L12	25.40	76.20	127.9	49.40	51.70	36.72	13.30	3.27	11.51
L13	50.80	93.66	183.3	39.40	101.9	66.03	8.00	1.99	9.31
L14	50.80	93.66	159.0	16.50	99.10	53.66	19.20	4.92	22.34
L15	50.80	93.66	213.2	92.00	97.90	46.93	16.70	4.33	19.43
D1	12.70	76.20	110.5	45.70	28.60	8.30	31.30	6.95	22.39
D2	12.70	76.20	116.2	43.20	31.80	8.57	34.20	6.83	24.43
D3	12.70	76.20	161.4	54.30	37.40	7.43	29.70	5.04	21.19
D4	12.70	76.20	155.0	70.10	29.40	6.17	22.10	4.77	15.80
D5	25.40	76.20	113.0	25.20	50.20	25.99	16.70	4.22	14.45
D6	25.40	76.20	130.3	41.50	47.00	17.62	22.00	5.94	19.06
D7	25.40	76.20	106.7	19.80	53.60	18.14	21.80	5.17	18.85
D8	50.80	93.66	118.3	11.30	80.70	40.83	11.00	3.46	12.81
D9	50.80	93.66	168.8	27.20	102.0	53.38	15.10	3.76	17.57
D10	50.80	93.66	199.0	42.60	97.50	40.36	14.50	3.78	16.87

a = plug radius, R = cylinder radius, L_r = cylinder length, L_h = length of the coaxial borehole above the cement plug, L = cement plug length, and M, L, D = medium, low, and dry saturation condition, respectively.

$$\sigma_{z,f} = 147.29a^{-0.5736};\ r = -0.962 \quad (11)$$

$$\sigma_{z,f} = 174.75a^{-0.6285};\ r = -0.760 \quad (12)$$

$$\sigma_{z,f} = 118.98a^{-0.5545};\ r = -0.910 \quad (13)$$

where $\sigma_{z,f}$ = axial strength (MPa), a = plug radius (mm), and r = correlation coefficient.

Fig. 2 and Eqs. (11) through (13) show that the axial strength decreases with increasing plug radius. The relation can be described quite well by a power law. The size effect

Table 3
Mean degree of saturation (±1 SD, %) of samples

	Tuff cylinder plug radius (mm)			
Push-out sample saturation condition	6.35	12.7	25.4	50.8
Medium	51.88 ± 2.88 (14)	54.57 ± 3.72 (6)	59.97 ± 5.46 (3)	72.99 ± 1.43 (3)
Low	–	24.29 ± 7.12 (7)	46.22 ± 7.70 (5)	61.61 ± 10.85 (3)
Dry	–	7.62 ± 1.08 (4)	20.58 ± 4.69 (3)	44.86 ± 7.39 (3)

The number of samples tested are given in parentheses.

Table 4
Mean axial strength (±1 SD, MPa) of samples

	Tuff cylinder plug radius (mm)			
Push-out sample saturation condition	6.35	12.7	25.4	50.8
Medium	50.53 ± 6.23 (14)	35.20 ± 4.40 (6)	22.70 ± 5.48 (3)	14.87 ± 1.67 (3)
Low	–	34.64 ± 6.43 (7)	26.40 ± 8.11 (5)	14.63 ± 5.88 (3)
Dry	–	29.33 ± 5.16 (4)	20.17 ± 3.00 (3)	13.53 ± 2.21 (3)

The number of samples tested are given in parentheses.

encountered on axial strength may be related to the size-strength studies performed on pillars (i.e., large rock blocks in mines) [36]. When a fracture occurs in a cubic pillar with a side length, L, a certain amount of strain energy, U, is required to satisfy the energy balance for each unit area of the fracture surface created. If the fracture results from brittle breakdown, and the strain energy per unit fracture area (U/L^2) is assumed to be constant, then the strength of the pillar is inversely proportional to the square root of one of the pillar linear dimensions (or the plug diameter in the case of a push-out specimen). This might explain the inverse proportionality between axial strength and plug radius.

The extrapolated axial strengths of the low and medium saturated samples to a plug radius of 100 mm are higher than that of the dry samples. Extrapolation of Eqs. (11) through (13) to an in situ plug of radius 2.50 m shows that the axial strength for the medium saturated, low saturated, and dry samples is 1.66, 1.28, and 1.55 MPa, respectively. This suggests that any extrapolation should be performed with caution and confirms the desirability of performing push-out tests on larger radius plugs in situ as a function of varying degrees of saturation of the host rock. This will aid in identifying size and saturation effects and in particular will provide insight to the validity of the power law extrapolation obtained through Eqs. (11) through (13).

Extensive experience with borehole plug testing [17–20,34,35,37,38] strongly indicates that frictional bonding is the most important, and in many rock types probably the only interaction between cementitious plugs and host rocks. Nevertheless, it is also recognized that in certain rock types, such as in highly siliceous welded tuff in which the push-out tests have been conducted, chemical interactions between

Table 5
Mean bond strength (±1 SD, MPa) of samples

	Tuff cylinder plug radius (mm)			
Push-out sample saturation condition	6.35	12.7	25.4	50.8
Medium	10.90 ± 1.24 (14)	7.33 ± 0.97 (6)	6.29 ± 1.89 (3)	3.93 ± 0.74 (3)
Low	–	7.57 ± 1.01 (7)	6.60 ± 2.03 (5)	3.74 ± 1.57 (3)
Dry	–	5.90 ± 1.15 (4)	5.11 ± 0.86 (3)	3.67 ± 0.18 (3)

The number of samples tested are given in parentheses.

Table 6
Mean peak shear strength (±1 SD, MPa) of samples

	Tuff cylinder plug radius (mm)			
Push-out sample saturation condition	6.35	12.7	25.4	50.8
Medium	36.14 ± 4.43 (14)	25.13 ± 3.15 (6)	19.68 ± 4.78 (3)	17.30 ± 1.94 (3)
Low	–	24.79 ± 6.43 (7)	22.85 ± 7.02 (5)	17.03 ± 6.84 (3)
Dry	–	20.95 ± 3.69 (4)	17.45 ± 2.62 (3)	15.75 ± 2.57 (3)

The number of samples tested are given in parentheses.

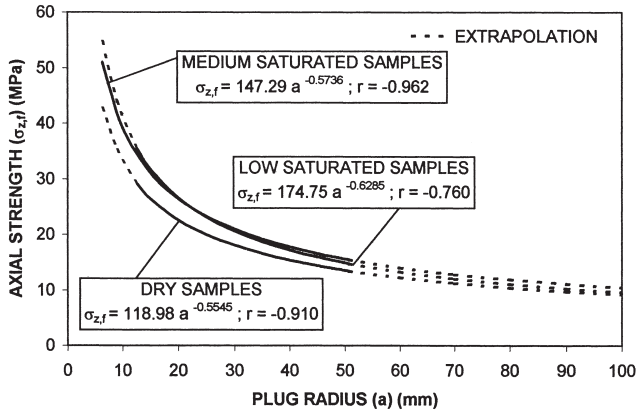

Fig. 2. Axial strength as a function of degree of saturation and plug radius.

cement grouts and host rock are likely [39–41]. However, for interface strength testing, analysis, and design purposes, all indications are that a simple mechanical friction bond is adequate and realistic.

This study made no attempt to predict the relation between axial strength and cement curing period. Push-out tests should be performed on cement plugs with a variety of relatively long curing times (i.e., months to years) to help identify any reactions that might take place between the plug, host rock, and water and whether rock-plug interactions are beneficial or detrimental, and to what extent.

References

[1] D.L. South, J.J.K. Daemen, Permeameter studies of water flow through cement and clay borehole seals in granite, basalt, and tuff, Tech. Rep., NUREG/CR-4748, U.S. Nuclear Regulatory Commission, Washington, D.C., 1986.

[2] D.M. Roy, M.W. Grutzeck, L.D. Wakeley, Salt repository seal materials: A synopsis of early cementitious materials development, Tech. Rep. BMI/ONWI-536, Office of Nuclear Waste Isolation, Battelle Memorial Institute, Columbus, OH, 1985.

[3] L.D. Wakeley, D.M. Roy, M.W. Grutzeck, Experimental studies of seal materials for potential use in a Los-Medanos type bedded salt repository, Tech. Rep. ONWI-325, Office of Nuclear Waste Isolation, Battelle Memorial Institute, Columbus, OH, 1981.

[4] D'Appolonia Consulting Engineers, Sealing considerations for repository shafts in bedded and dome salt, Tech. Rep. ONWI-255, Office of Nuclear Waste Isolation, Battelle Memorial Institute, Columbus, OH, 1981.

[5] W.E. Coons, D. Meyer, P.C. Kelsall, Evaluation of polymer concrete for application to repository sealing, Tech. Rep. ONWI-410, Office of Nuclear Waste Isolation, Battelle Memorial Institute, Columbus, OH, 1982.

[6] K. Fuenkajorn, J.J.K. Daemen (Eds.), Sealing of Boreholes and Underground Excavations in Rock, Chapman & Hall, London, 1996.

[7] C.W. Gulick Jr., J.A. Boa, Jr., A.D. Buck, Bell Canyon Test—Cement development report, Proc. Workshop on Borehole and Shaft Plugging, Columbus, OH, 1980, pp. 277–296.

[8] C.W. Gulick Jr., J.A. Boa Jr., A.D. Buck, Bell Canyon Test (BCT) cement grout development report, Tech. Rep. SAND80-1928, Sandia National Laboratories, Albuquerque, NM, 1980.

[9] P.C. Kelsall, W.E. Coons, D. Meyer, Repository sealing program plan: Repository in salt, Tech. Rep. ONWI-414, Office of Nuclear Waste Isolation, Battelle Memorial Institute, Columbus, OH, 1983.

[10] L.D. Wakeley, D.M. Walley, A.D. Buck, Development of a freshwater grout subsequent to the Bell Canyon Tests (BCT), Misc. Paper SL-85-2, Sandia National Laboratories, Albuquerque, NM, 1986.

[11] R. Malinowski, Ancient mortars and concretes: Aspects of their durability, in: A.R. Hall, N. Smith (Eds.), History of Technology, 7th Ann. Vol., Mansell Publishing Ltd., London, 1982, pp. 89–100.

[12] J.G. Moore, M.T. Morgan, E.W. McDaniel, H.B. Greene, G.A. West, Cement technology for plugging boreholes in radioactive waste repository sites, Progress Rep. ORNL-5524, Oak Ridge National Laboratory, Oak Ridge, TN, 1978.

[13] D.M. Roy, C.A. Langton, Characterization of cement-based ancient building materials in support of repository seal materials studies, Tech. Rep. BMI/ONWI-523, Office of Nuclear Waste Isolation, Battelle Memorial Institute, Columbus, OH, 1983.

[14] J.E. Rhoderick, Examination of a sample of grout after 63 years exposure underground, Tech. Rep. ONWI-248, Office of Nuclear Waste Isolation, Battelle Memorial Institute, Columbus, OH, 1981.

[15] A.D. Buck, J.P. Burkes, Examination of grout and rock from Duval Mine, New Mexico, Misc. Paper SL-79-6, U.S. Army Engineer Waterways Experiment Station, Vicksburg, MS, 1979.

[16] H. Akgün, Strength parameters of cement borehole seals in rock, in: K. Fuenkajorn, J.J.K. Daemen (Eds.), Sealing of Boreholes and Underground Excavations in Rock, Chapman & Hall, London, 1996, pp. 28–39.

[17] H. Akgün, An assessment of borehole sealing performance in a salt environment, Environmental Geology 31 (1–2) (1997) 33–41.

[18] H. Akgün, J.J.K. Daemen, Bond strength of cementitious borehole plugs in welded tuff, Tech. Rep. NUREG/CR-4295, U.S. Nuclear Regulatory Commission, Washington, D.C., 1991.

[19] H. Akgün, J.J.K. Daemen, Analytical and experimental assessment of mechanical borehole sealing performance in rock, Engineering Geology 47 (1997) 233–241.

[20] H. Akgün, J.J.K. Daemen, Design implications of analytical and laboratory studies of permanent abandonment plugs, Canadian Geotechnical Journal 36 (1999) 21–38.

[21] D.M. Roy, M.W. Grutzeck, L.D. Wakeley, Selection and durability of seal materials for a bedded salt repository: Preliminary studies, Tech. Rep. ONWI-479, Office of Nuclear Waste Isolation, Battelle Memorial Institute, Columbus, OH, 1983.

[22] L.D. Wakeley, D.M. Roy, Cementitious mixtures for sealing evaporite and clastic rocks in a radioactive-waste repository, Misc. Paper SL-85-16, Office of Nuclear Waste Isolation, Battelle Memorial Institute, Columbus, OH, 1985.

[23] L.D. Wakeley, D.M. Roy, M.W. Grutzeck, Cementitious mixtures for sealing access shafts/boreholes through evaporite and clastic rocks in a radioactive-waste repository, in: C.M. Jantzen, J.A. Stone, R.C. Ewing (Eds.), Scientific Basis for Nuclear Waste Management VIII, Materials Research Soc. Symp. Proc., Pittsburgh, PA, Vol. 44, 1985, pp. 951–958.

[24] L.D. Wakeley, D.M. Roy, Nature of the interfacial region between cementitious mixtures and rocks from the Palo Duro Basin and other seal components, Tech. Rep. BMI/ONWI-580, Office of Nuclear Waste Isolation, Battelle Memorial Institute, Columbus, OH, 1986.

[25] L.L. Van Sambeek, Thermal and thermomechanical analysis of WIPP shaft seals, Tech. Rep. RSI-0324, Sandia National Laboratories, Albuquerque, NM, 1987.

[26] H. Jezierski, Dam construction in salt formations, Proc. Symp. Waste Management 2 (1984) 261–267.

[27] D.G. Calvert, Shrinkage-compensating cements in oil well cementing. Pub. SP-64, American Concrete Institute, Detroit, MI, 1980, pp. 193–197.

[28] J.E. Rhoderick, A.D. Buck, Examination of simulated borehole specimens, Tech. Rep. ONWI-247, Office of Nuclear Waste Isolation, Battelle Memorial Institute, Columbus, OH, 1981.

[29] D.M. Roy, M.W. Grutzeck, P.H. Licastro, Evaluation of cement borehole longevity, Tech. Rep. ONWI-30, Office of Nuclear Waste Isolation, Battelle Memorial Institute, Columbus, OH, 1979.

[30] K. Fuenkajorn, J.J.K. Daemen, Mechanical characterization of densely welded Apache Leap Tuff, Tech. Rep. NUREG/CR-5688, U.S. Nuclear Regulatory Commission, Washington, D.C., 1991.
[31] ASTM D2938-79, Standard test method for unconfined compressive strength of intact rock core specimens, 04.08, 1979.
[32] American Petroleum Institute, Specifications for materials and testing for well cements, API Spec. 10, 4th Ed., API, Washington, D.C., 1988, p. 103.
[33] G. Adisoma, J.J.K. Daemen, Experimental assessment of the influence of dynamic loading on the permeability of wet and of dried cement borehole seals, Tech. Rep. NUREG/CR-5129, U.S. Nuclear Regulatory Commission, Washington, D.C., 1988.
[34] H. Akgün, J.J.K. Daemen, Size influence on the sealing performance of cementitious borehole plugs, Tech. Rep. NUREG/CR-4738, U.S. Nuclear Regulatory Commission, Washington, D.C., 1986.
[35] H. Akgün, J.J.K. Daemen, Performance assessment of cement grout borehole plugs in basalt, Engineering Geology 37 (1994) 137–148.
[36] I.W. Farmer, Coal Mine Structures, Chapman & Hall, London, 1985.
[37] J.C. Stormont, J.J.K. Daemen, Axial strength of cement borehole plugs in granite and basalt, Topical Rep. NUREG/CR-3594, U.S. Nuclear Regulatory Commission, Washington, D.C., 1983.
[38] W.B. Greer, J.J.K. Daemen, Analyses of field tests of the hydraulic performance of cement grout borehole seals. Tech. Rep. NUREG/CR-5684, U.S. Nuclear Regulatory Commission, Washington, D.C., 1991.
[39] B.E. Scheetz, D.M. Roy, Geochemical performance evaluation and characterization of a potential cementitious repository sealing material for application in the Topopah Spring Tuff NNWSI investigations, in: C.M. Jantzen, J.A. Stone, R.C. Ewing (Eds.), Scientific Basis for Nuclear Waste Management VIII, Materials Research Soc. Symp. Proc., Pittsburgh, PA, Vol. 44, 1985, pp. 935–942.
[40] R.I.A. Malek, D.M. Roy, Dissolution kinetics of tuff rock and mechanism of chemical bond formation at the interface with cement grout, in: C.M. Jantzen, J.A. Stone, R.C. Ewing (Eds.), Scientific Basis for Nuclear Waste Management VIII, Materials Research Soc. Symp. Proc., Pittsburgh, PA, Vol. 44, 1985, pp. 943–950.
[41] P.K. Mehta, P.J.M. Monteiro, Concrete Structure, Properties, and Materials, 2d ed., Prentice-Hall, Englewood Cliffs, NJ, 1986.